

Mobility Strategies based on Virtual Forces for Swarms of Autonomous UAVs in Constrained Environments

Ema Falomir, Serge Chaumette, Gilles Guerrini

► **To cite this version:**

Ema Falomir, Serge Chaumette, Gilles Guerrini. Mobility Strategies based on Virtual Forces for Swarms of Autonomous UAVs in Constrained Environments. International Conference on Informatics in Control, Automation and Robotics (ICINCO 2017), Jul 2017, Madrid, Spain. pp.221-229. hal-01530393v2

HAL Id: hal-01530393

<https://hal.archives-ouvertes.fr/hal-01530393v2>

Submitted on 3 Jul 2018

HAL is a multi-disciplinary open access archive for the deposit and dissemination of scientific research documents, whether they are published or not. The documents may come from teaching and research institutions in France or abroad, or from public or private research centers.

L'archive ouverte pluridisciplinaire **HAL**, est destinée au dépôt et à la diffusion de documents scientifiques de niveau recherche, publiés ou non, émanant des établissements d'enseignement et de recherche français ou étrangers, des laboratoires publics ou privés.

Mobility Strategies based on Virtual Forces for Swarms of Autonomous UAVs in Constrained Environments

Ema Falomir^{1,2}, Serge Chaumette¹ and Gilles Guerrini²

¹Bordeaux Computer Science Research Laboratory, Bordeaux University, Talence, France

²Thales Systèmes Aéroportés, Mérignac, France

{ema.falomir-bagdassarian, serge.chaumette}@labri.fr, {ema.falomir, gilles.guerrini}@fr.thalesgroup.com

Keywords: UAV, Swarm, Autonomous Swarm of UAVs, Compactness, Virtual Forces, Distributed Robotic Systems.

Abstract: The usage of autonomous unmanned aerial vehicles (UAVs) has recently become a major question. For wide area surveillance missions, a swarm of UAVs can be much more efficient than a single vehicle. In this case, several aircrafts cooperate in order to fulfill a mission while avoiding collisions between each other and with obstacles. This article proposes original distributed mobility strategies for autonomous swarms of UAVs, the goal of which is to fulfill a surveillance mission. Our work is based on virtual forces and our approach allows narrow areas crossing that require a compact formation of the autonomous swarm.

1 INTRODUCTION

In the past few years, the usage of unmanned aerial vehicles (UAVs) has been widely studied. In this paper, we consider rotor wings, which allow low speed maneuvering and hovering.

A set of several UAVs deployed on the same area, independent of any infrastructure and able to establish peer-to-peer connections form a flying ad-hoc network (FANET) (Bekmezci et al., 2013). A FANET offers several advantages in comparison to a single UAV. Additionally to a larger coverage, if one aircraft of a FANET encounters a failure, the assigned mission can still be achieved. Furthermore, each UAV can embed a different sensor, which could not fit inside a single aircraft.

Several studies have already been carried out on surveillance missions lead by FANETs. The UAVs can all be multirotors (Chaumette et al., 2011) but multirotors also can be associated with fixed-wings (Jaimes et al., 2008), (Bouvry et al., 2016).

In this paper, we will consider a FANET composed of multirotors with the same kinematics characteristics, able to fulfill a mission autonomously. We will refer to this particular kind of FANET as “autonomous swarm”. In this configuration, an operator only deals with a single entity contrary to a multiplatform system.

To evolve in partially unknown environment autonomously, the UAVs have to calculate their

flight plans online. Here, not to be dependent of a single UAV, each one calculates its own flight plan.

Methods based on artificial potential fields (introduced in (Khatib, 1986)) are often chosen for online and decentralized applications thanks to their limited needs in terms of computation and because they are distributed by nature. They can be used to maximize area coverage (Howard et al., 2002), (Gobel and Krzesinski, 2008) or to obtain specific connectivity characteristics (Casteigts et al., 2012). Some studies also aim at reaching a target with robot cars thanks to artificial forces approaches (Boonyarak and Prempraneerach, 2014), (Jin et al., 2014) but these methods have not been widely extended to swarms.

In this paper, we consider a cooperative and autonomous swarm of multirotors in the context of a surveillance mission of two areas of interest (AoIs), as represented on the Figure 1. The two AoIs are separated by a narrow passage (a tunnel), possibly containing static obstacles of unknown position and size, requiring a compact formation of the swarm.

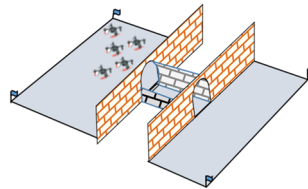


Figure 1: Representation of the two Areas of Interest separated by a narrow passage (a tunnel).

We propose a new distributed mobility strategy for autonomous swarms of UAVs, based on virtual forces in order to avoid collisions between the UAVs and with obstacles, and maximize the communication links along a surveillance mission.

The remainder of this paper is organized as follows. Section 2 presents the scenario and the associated hypothesis. Section 3 introduces the forces used in the mobility strategies thereafter presented in section 4. Section 5 introduces the metrics used to evaluate the efficiency of our mobility strategies. The results are shown in section 6. Finally, section 7 is dedicated to the conclusion of this work and sketches future research directions.

2 SCENARIO AND HYPOTHESIS

2.1 Scenario

Our mission aims at the successive surveillance, by an autonomous swarm of UAVs, of two AoIs separated by a narrow passage possibly containing obstacles unknown prior to the mission. The UAVs are multicopters equipped with limited range sensors supporting the surveillance mission and allowing obstacle detection and with communication systems.

2.2 Hypothesis

We suppose that there are no obstacles in the AoIs but only in the narrow passage which is the phase of the scenario that we want to study in details. We also assume consider that the UAVs know the coordinates of the AoIs corners and of the passage entrance. Additionally, it is supposed that no UAV is added or removed from the system.

As we are interested in mobility strategies, we do not consider neither “low-level” details in this first study (communication protocols, localization, etc.) nor the UAVs flight dynamics. Moreover, it is supposed that the UAVs have enough energy to fulfill the complete mission.

3 CONTRIBUTION 1: VIRTUAL FORCES

To achieve a surveillance mission and to avoid collisions, mobility strategies are proposed based on virtual forces and on distances of interest which are presented in the following subsections.

For this study, we have chosen to define the forces with a magnitude comprised between -1 and 1. Attractive forces are positive, repulsive forces are negative. This permits to easily compare the influence of several forces in a system which can be complex. Moreover, as this is a preliminary study, forces are defined on the basis of linear functions.

3.1 Safety Distance

In order to avoid collisions, a minimal safety distance, D_{safe} has to be maintained between each UAV and other objects. For this preliminary study, we define this distance as follows:

$$D_{safe} = 1.5 \times UAV_{size} \quad (1)$$

3.2 Inter-UAV Wanted Distance

During the mission, two goals must be achieved. First, the maintenance of the communication links, and second the coverage of the AoI with little redundancy. Consequently, we define an inter-UAV wanted distance which takes into account the communication and the surveillance sensor ranges:

$$D_{int} = k \times \min(2 r_{sensor}, r_{communication}) \quad (2)$$

where $k \in]0; 1[$.

It is important to note that D_{int} must be greater than (or equal to) D_{safe} to use the strategy described in the following sections. In practice, this condition is not limiting as UAVs always embed sensors with range larger than their own size.

3.3 Attraction-repulsion between UAVs

To fulfill their mission, the UAVs should remain spaced of D_{int} . In this aim, an attractive force is applied when they are further and a repulsive one when they are closer, depending on their distance d_{UU} . As the UAVs safety is more important than the mission accomplishment, the repulsive forces have to be stronger than the attractive ones. The attractive-repulsive virtual forces between UAVs are directed from the considered UAV to its neighbor and of magnitude F_{ar} (see Figure 2) defined in (3).

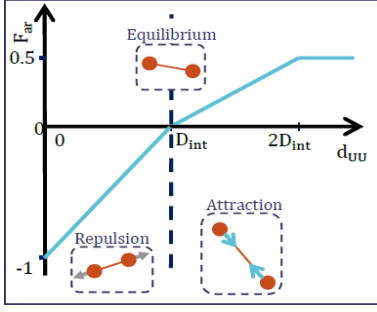


Figure 2: Graphical representation of the attractive-repulsive force between UAVs. On the schemes, UAVs are represented by open and triangle arrows respectively. The lines linking the UAVs represent communication links. *Note: These notations will be used all along the paper.*

$$F_{ar} = \begin{cases} \frac{1}{D_{int}} d_{UV} - 1 & \text{if } d_{UV} < D_{int} \\ 0.5 & \text{if } d_{UV} > 2D_{int} \\ \frac{1}{2} \left(\frac{d_{UV}}{D_{int}} - 1 \right) & \text{else} \end{cases} \quad (3)$$

3.4 Attraction towards a Goal

To fulfill the mission, the UAVs have to deploy on the AoIs, fly over them, and cross the passage. To achieve these goals, each UAV calculates temporary targets all along the mission and is subject to an attractive force towards them.

We have chosen to give a constant magnitude to the attractive force towards a goal till a certain distance. In the area around the target, the force decreases linearly with respect to the robot-goal distance d_g , in order to avoid oscillations around the goal. This decrease near the target also favors the other forces in this area.

The attraction to a goal is directed towards the goal and is of magnitude F_g (represented on Figure 3) defined as follows:

$$F_g = \begin{cases} 0.5 & \text{if } d_g > D_{int} \\ \frac{d_g}{2D_{int}} & \text{else} \end{cases} \quad (4)$$

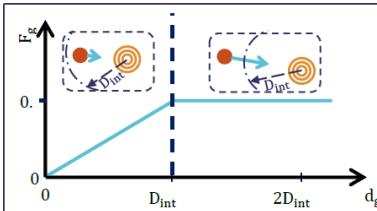


Figure 3: Graphical representation of the attractive force to a goal. The UAV target is represented by nested circles. *Note: This notation will be used all along this paper.*

3.5 Repulsion Due to Obstacles

The repulsion due to obstacles is based on the safety distance D_{safe} . In this first study, we admitted that if a UAV is further away than three times its safety distance from an obstacle, it should not consider the obstacle. Nonetheless, in future work this repulsive force should be based on other characteristics.

The repulsive force due to an obstacle is directed at the opposite of the obstacle. A first magnitude has been tested, F_{obs}^1 , defined as follows:

$$F_{obs}^1 = \begin{cases} \frac{d_{obs}}{3D_{safe}} - 1 & \text{if } d_{obs} < 3D_{safe} \\ 0 & \text{else} \end{cases} \quad (5)$$

where d_{obs} is the UAV-obstacle distance. Using this first approach, the repulsion due to obstacles was too high compared to the attraction-repulsion between UAVs. As a result, the swarm did not remain connected in the tunnel, and collisions between UAVs occurred. Indeed, between $2D_{safe}$ and $3D_{safe}$, the obstacle had a too high influence. So we modified the magnitude to F_{obs} , represented in the Figure 4, defined as follows:

$$F_{obs} = \begin{cases} 0 & \text{if } d_{obs} > 3D_{safe} \\ \frac{9}{20} \times \frac{d_{obs}}{D_{safe}} - 1 & \text{if } d_{obs} < 2D_{safe} \\ \frac{1}{10} \left(\frac{d_{obs}}{D_{safe}} - 3 \right) & \text{else} \end{cases} \quad (6)$$

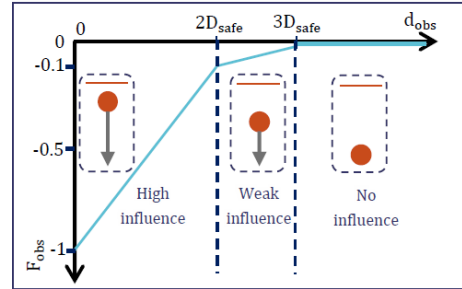


Figure 4: Graphical representation of the repulsive force due to obstacles. The obstacle is represented by a line.

3.6 Weighted Average

At each step, each UAV is subject to several virtual forces as illustrated on the Figure 5. UAVs calculate a weighted average of all the virtual forces applied to them and their next direction is resulting of this weighted average. The weight of each force is the exponential of its magnitude, as proposed for spring forces in a work on network biconnection (Casteigts et al., 2012).

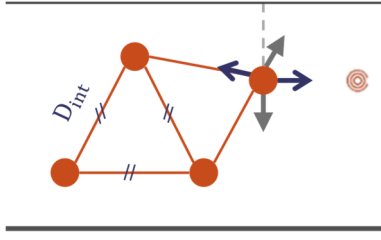


Figure 5: Scheme of the repulsive and attractive forces applied to a UAV in a swarm, in a narrow passage.

4 CONTRIBUTION 2: MOBILITY STRATEGIES

As introduced in section 2, our scenario is composed of three main phases: survey the AoIs, make-up of the compact formation and cross the tunnel. In the following subsections we detail the mobility strategies for each of these three steps.

4.1 Surveillance Mobility Strategy

During the surveillance phase, each UAV should have, at each moment, a vision of the whole AoI as recent as possible. To be able to build this view in a cooperative manner, the UAVs have to be deployed all over the area and maintain communication links.

An adapted mobility strategy consists in creating an “S-shaped” travel over the AoI, as illustrated in Figure 6. The mesh to support the movements of the UAVs is calculated at the very beginning of the mission and is composed of cells of size $D_{int} \times D_{int}$.

In this mobility strategy, the targets of the UAVs are located at the extremity of the lines. Once a UAV reaches its temporary goal, it calculates its next target, depending on its identifier and of the number of vehicles in the swarm. Its move towards this target starts when its 1- and 2-hop neighbors have reached their own goals. In this way, the connectivity of the swarm is maintained.

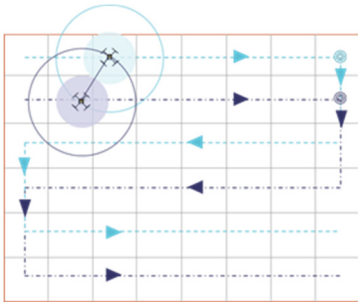


Figure 6: Movements of a swarm composed of two UAVs during the surveillance mission over an AoI.

During the surveillance, each UAV is subject to attractive-repulsive force with its neighbors and to attractive force towards its successive targets.

4.2 Compact Swarm Formation Setup

Once the first AoI has been covered, the swarm flies toward the passage in which it can encounter obstacles. In this study, the UAVs do not share the obstacles location, but in a further work this should be implemented. To facilitate this, a biconnectivity of the swarm is sought. In case of a very narrow passage (*i.e.* of a width smaller than $3D_{safe}$), UAVs can only get through the tunnel in a queue (Figure 7 a), so biconnectivity cannot be guaranteed. Else, the swarm can organize itself in a staggered rows formation (see Figure 7 b) and c)). The 2-row staggered formation can be setup when the passage width is greater than $2D_{safe} + \sqrt{3}/2D_{int}$. To allow 3 rows, the tunnel width has to be greater than $2D_{safe} + \sqrt{3}D_{int}$. These values can easily be geometrically calculated.

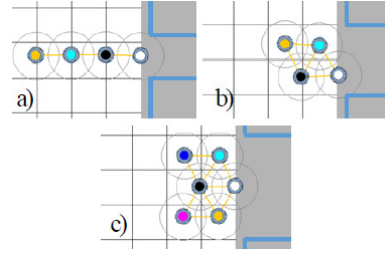


Figure 7: a) Too narrow passage for a biconnectivity. This will be referred to as Tunnel shape a. b) 2-row staggered biconnected formation. (Tunnel shape b.) c) Biconnected formation for larger passages. (Tunnel shape c.).

From the passage width, the number of vehicles in the swarm and its identifier, each UAV calculates a target close to the tunnel entrance, in a deterministic manner. The connectivity of the swarm during the surveillance ensures that all the UAVs know when they have to go towards the tunnel entrance. The positions of the UAVs in compact formation are separated of D_{int} , so there will be some communication links between the UAVs. So, only the repulsive forces between the UAVs and the attractive force to their goal are necessary when the swarm travels towards the tunnel entrance. The swarm starts to get through the passage only when all the UAVs are at their position or when UAVs are at their correct location for a defined duration.

4.3 Passage Crossing Mobility Strategy

The swarm has to cross the tunnel to reach the second AoI.

When the UAVs get through the tunnel, they are subject to the virtual attractive-repulsive forces between each other, the repulsive force due to the obstacles and the attractive force towards a goal. As the UAVs do not know the shape of the passage, they calculate at each step a new temporary target in the direction of the second AoI. This target is located at a small distance (we arbitrarily chose $D_{int}/4$) and so produces a weak attraction, the goal being to favor collision avoidance and to maintain of the communication links.

If an obstacle is located between the UAV and its target, the UAV stops being attracted towards this point and it favors the attraction towards its neighbors so as not to stay in a local minima.

We consider that the UAVs can communicate even if an obstacle is located between them. Additionally, if a UAV shares a communication link with another one in the opposite direction of its target and if an obstacle is between them, the first UAV will not take into account the attractive force towards this neighbor (see Figure 8). A further simplification is made in this first study concerning the repulsion due to obstacles. Each UAV decomposes its environment in four equal areas: upper, below, backwards and ahead. They take into account a maximum of one repulsive force due to obstacles in each quadrant. If several obstacles are in a same quadrant, the closest one only is taken into account. This is enough to avoid obstacles.

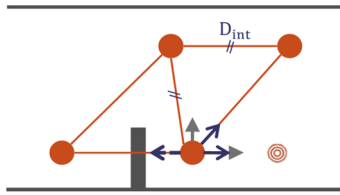


Figure 8: Case when an attractive force is not taken into account (dotted open arrow). The forces are plotted for the UAV of interest.

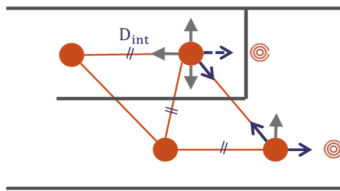


Figure 9: A limitation of the model. The forces are plotted for only two UAVs for the sake of visibility. The two upper UAVs do not go backward for joining the others.

Nonetheless, limitations exist. Indeed, there is no definition of a new target if there is an obstacle between it and the UAV, and favoring the attraction towards other UAVs is not always sufficient as illustrated on Figure 9.

5 EVALUATION CRITERIA

The presents the Measures of Performance (MoPs) for the three parts of the scenario. For each MoP, an ideal result is given, not always achievable.

6 SIMULATION AND RESULTS

The following subsections present the simulation tool used in this study, the parameters of the simulations and the results for the different steps, according to the MOPs defined in section 5.

6.1 JBotSim Simulation Tool

To simulate the mobility strategies defined in the previous section, we chose the open source simulation library JBotSim (Casteigts, 2015). It is a tool for distributed algorithms fast prototyping in dynamic networks. Contrary to other well-known simulators such as NS3 (Riley and Henderson, 2010) or OMNet++ (Varga, 2001), JBotSim does not implement real-world networking protocols, which was not required in this preliminary study.

6.2 Simulation Scenario and Parameters

We have conducted a series of simulation to validate our mobility strategies. For all the simulations the k factor used in the D_{int} definition is fixed at 0.75.

We chose to simulate UAVs of circular shapes of 20cm diameter, equipped with a communication system of 1.10m range and with a sensor used for both surveillance and obstacle detection of 50cm range.

The first AoI is 9m long and 7.50m large. At each simulation step, the UAVs travel at a random distance comprised between 5cm and 10cm in the resulting direction of the virtual forces average.

Table 1: Evaluation criteria and ideal result for each step of the mission.

	Operational Objective	MoPs	Ideal Result
Overall mission	Safeguard of the UAV	<ul style="list-style-type: none"> ▪ Distance between a UAV and another object 	<ul style="list-style-type: none"> ▪ Greater than a given safety distance
Surveillance mission	Deploy over the AoI with communication links	<ul style="list-style-type: none"> ▪ Duration of an AoI coverage ▪ Number of disconnections ▪ Number of connections 	<ul style="list-style-type: none"> ▪ Inversely proportional to the number of UAVs ▪ None ▪ Equal to the number of disconnections
Compact formation setup	Quick set up before crossing the tunnel	<ul style="list-style-type: none"> ▪ Duration of compact formation setup 	<ul style="list-style-type: none"> ▪ Time of travel between the furthest UAV and the tunnel entrance, by the shortest path
Tunnel crossing	Join the second AoI while avoiding collisions	<ul style="list-style-type: none"> ▪ Duration of tunnel crossing ▪ Number of network disconnections ▪ Number of network re-connections 	<ul style="list-style-type: none"> ▪ Time of travel of one UAV in the tunnel by the shortest path ▪ None ▪ Equal to the number of disconnections

A view of the AoIs, tunnel and UAVs extracted from JBotSim is shown on the Figure 10.

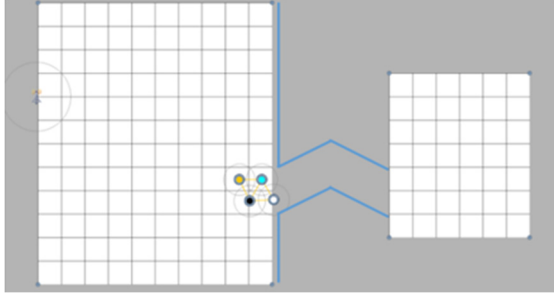


Figure 10: View of the two AoIs and of the passage referred to as Tunnel d.

Simulations have been performed with swarms composed of 1 to 6 UAVs and with 5 tunnels (see Figure 7, Figure 10 and Figure 11). For each parameter set we have run 30 simulations. At the entrance, shape a tunnel is 95cm large, tunnels b, d and e are 151cm large and finally tunnel c is 226cm large.

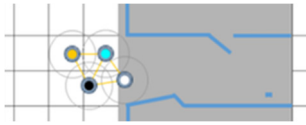


Figure 11: Passage referred as Tunnel e.

6.3 Simulation Results, Evaluation and Analysis

6.3.1 Overall Mission

During the whole mission, the priority is to safeguard the UAVs. To achieve this goal, the distance between a UAV and another object has to remain above the safety distance defined previously.

The minimal distance between the UAVs as well

as between the UAVs and an obstacle, remained above 1.3 times D_{safe} , for all the simulation ran. Thus, the main objective of the project is reached.

6.3.2 Surveillance

As expected, the simulations have shown that the more UAVs compose the swarm, the quicker the complete surveillance is performed (see Table 2).

The very small difference of duration between 4 and 5 UAVs is due to the number of rows of the mesh supporting the UAVs movements in the AoI. Indeed, a 4-UAV swarm has to cross the 12-row area three times to fully cover it, as a 5-UAV swarm.

Furthermore, a UAV moves towards its next target only when its neighbors have reached their own one. Indeed the more UAVs compose the swarm, the higher is the probability to have to wait for other UAVs. This is why the speed-up, defined as follows, is not linear:

$$\text{SpeedUp}(n \text{ UAVs}) = \frac{\text{duration (1 UAV)}}{\text{duration (n UAVs)}} \quad (7)$$

Even if the objective of measuring a linear speed-up is not reached, we can observe a clear decrease in duration when the number of UAVs increases.

Table 2: Mean and standard deviation (SD) of the first AoI surveillance duration for various numbers of UAVs in the swarm, calculated on 150 runs for each number of UAVs.

Number of UAVs	Duration of surveillance (number of steps)		Speed Up
	Mean	SD	
1	1210	7	1
2	764	14	1.6
3	555	5	2.2
4	425	8	2.8
5	416	4	2.9
6	233	11	5.2

Finally, as the mobility strategy for the surveillance phase is almost deterministic (random speed of the UAVs), the standard deviation is low and so an estimation of the surveillance duration can be done by running a configuration only once.

Furthermore, we studied the creation and loss of links during the surveillance step (see the values in Table 3). We can see that there are on average a few loss of links, and as many creation as loss. The objective for this MOP is thus reached.

Table 3: Mean and standard deviation (SD) of the number of links lost and created during the surveillance phase, calculated on 150 runs for each number of UAVs.

Number of UAVs	Lost Links		Created Links	
	Mean	SD	Mean	SD
2	0.05	0.26	0.05	0.26
3	0.09	0.29	0.09	0.30
4	0.77	2.33	0.76	2.32
5	2.03	4.80	2.02	4.77
6	3.51	5.41	4.49	5.32

6.3.3 Compact Formation Setup

The Figure 12 shows the duration between the end of the surveillance and the moment when the compact formation is set up, normalized by the necessary time to go from the further UAV position to the tunnel entrance. As UAV target is not exactly at the tunnel entrance, the normalization can be smaller than one.

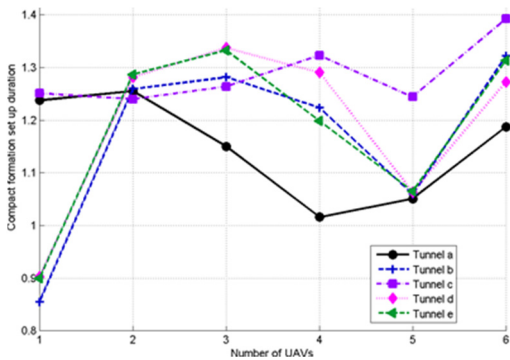


Figure 12: Mean compact formation setup duration for each simulated configuration, normalized.

Width of tunnel shape b, d and e are the same, so we wait for an identical duration of compact formation setting up. Nevertheless, differences appear between the 3 curves, due to the zoom effect.

In the case of a single UAV, the duration is the smallest for all the tunnels, because there is no repulsive force with neighbors, and so the UAV is not subject to forces opposed to the target attraction.

For all the configurations, the normalized compact formation setup duration is smaller than 1.4, which is a good result. This means that even for a swarm composed of numerous UAVs, and independently of the compact formation shape, the formation setup is rather quick.

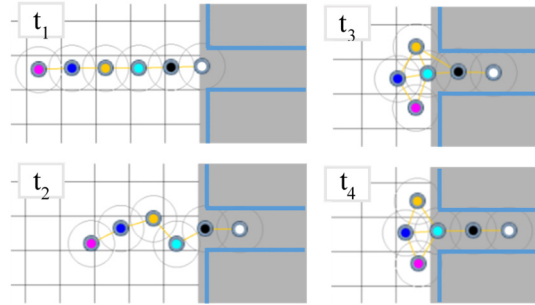


Figure 13: Movements of a 6-UAV swarm aiming at entering in the tunnel. At the time t_4 , the swarm is in a local equilibrium at the tunnel entrance.

We note that we tried to simulate a thinner width for Tunnel shape a (of width $2D_{safe}$ instead of $3D_{safe}$). In this case, only multi-UAVs swarms entered: for a single UAV, the repulsive forces at the entrance of the tunnel were greater than the attractive force towards the target. In the case of several UAVs, the attraction-repulsion between them was in the same direction as the attraction towards their target, which allowed the swarm to enter in the tunnel. Nevertheless it occurred that a 6-UAV swarm reached a local equilibrium at the passage entrance (see the progression of the swarm on Figure 13). In the case of such equilibrium, the closest UAVs to the tunnel were slowed down because of the repulsion due to the walls, while the other UAVs had a strong attraction towards their target and so did not remain behind the others.

6.3.4 Tunnel Crossing

The duration of tunnel crossing is the duration between the entrance of the first UAV and the exit of the last one. Results are represented in Figure 14.

The tunnel crossing duration for the thinner tunnel does not vary in function of the number of UAVs. This is because the UAVs have to be queued in this case and so the attractive-repulsive forces between them are in the direction of their target.

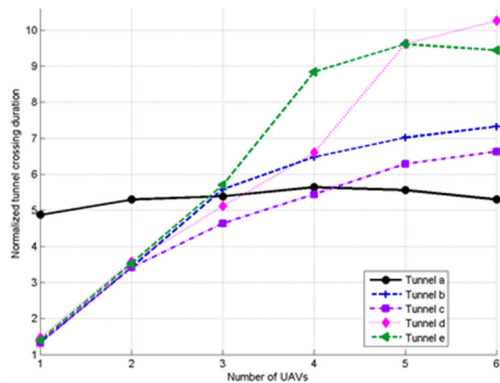


Figure 14: Tunnel crossing duration for each simulated configuration, normalized by the duration of tunnel crossing by a single UAV by the shortest path at maximum speed.

As expected, tunnels of shape b and c show the same trend even if the largest one is crossed quicker.

We note that in the case of several UAVs and tunnel of shape b to e, the crossing duration is longer than for a single UAV. This is due to the attractive-repulsive forces between the UAVs which are not in the direction of their target.

For the tunnel shape d, the crossing duration follows the trend of tunnel shapes b and c until 4 UAVs and skyrockets for 5 UAVs. This is due to the creation of additional links between the UAVs during the travel through the linear parts which have to be broken to pass over the corner.

In the case of the tunnel shape e, we can notice a strong increase of the crossing duration from 4 UAVs, due to the two obstacles which are too close to allow a biconnectivity. For that reason, some links between the UAVs have to be broken, while an attractive force between them is still applied. From 4 UAVs, two links have to be broken and only one in the case of 3 UAVs.

Moreover, in all the simulations, the connectivity of the swarm was maintained in the tunnel.

7 CONCLUSIONS AND FUTURE WORK

In this paper we propose original mobility strategies based on virtual forces for a swarm of autonomous UAVs. Following these strategies, the UAVs, all having equivalent roles, can autonomously fulfill a surveillance mission of two AoIs separated by a narrow passage. To travel from the initial AoI to the other, the swarm organizes itself as a compact formation favoring communication links between

the UAVs, which travel through the tunnel while avoiding obstacles unknown prior to the mission.

We have run many simulations and evaluated them using a number of criteria. Our results show that our approach gives very good results.

Nevertheless, numerous topics have to be further explored. First of all, the UAV safety distance should depend on the range of the embedded sensor used to detect the obstacles, as well as on the speed of the UAVs. Furthermore, each UAV that detects an obstacle should share its location with the other aircrafts of the swarm. Thanks to this information, the UAVs could calculate a new target points taking the obstacle into consideration. The presence of obstacles on the AoI could also be considered. A wide subject of study could be the self-organization of the swarm in order to make up a compact formation depending on the tunnel width, instead of the deterministic configuration presented in this work. Finally, magnitudes of the three forces could be defined by other functions, as polynomial or exponential. This could improve the model strategies by speeding up surveillance or tunnel crossing.

REFERENCES

- Al Redwan Newaz, A., Lee, G., Adi Pratama, F. & Young Chong, N., 2013. *3D Exploration Priority Based Flocking of UAVs*. Takamatsu, Japan, IEEE, pp. 1534-1589.
- Autefage, V., Chaumette, S. & Magoni, D., 2015. *A Mission-Oriented Service Discovery Mechanism for Highly Dynamic Autonomous Swarms of Unmanned Systems*. s.l., IEEE, pp. 31-40.
- Bekmezci, I., Sahingoz, O. K. & Temel, S., 2013. Flying Ad-Hoc Networks (FANETs): A survey. *Ad Hoc Networks*, May, 11(3), pp. 1254-1270.
- Boonyarak, S. & Prempraneerach, P., 2014. *Real-Time Obstacle Avoidance for Car Robot Using Potential Field and Local Incremental Planning*. Nakhon Ratchasima, Thailand, IEEE.
- Bouvry, P. et al., 2016. *Using heterogeneous multilevel swarms of UAVs and high-level data fusion to support situation management in surveillance scenarios*. Baden-Baden, IEEE, pp. 424-429.
- Cakir, M., 2015. *2D Path Planning of UAVs with Genetic Algorithm in a Constrained Environment*. Istanbul, Turkey, IEEE.
- Camp, T., Boleng, J. & Davies, V., 2002. A survey of mobility models for ad hoc network research. *Wireless Communications and Mobile Computing*, August, 2(5), pp. 483-502.
- Casteigts, A., 2015. *JBotSim: a Tool for Fast Prototyping of Distributed Algorithms in Dynamic Networks*. Athens, Greece, s.n.

- Casteigts, A. et al., 2012. Biconnecting a Network of Mobile Robots using Virtual Angular Forces. *Computer Communications*, 35(9), pp. 1038-1046.
- Chaumette, S. et al., 2011. *CARUS, an operational retasking application for a swarm of autonomous UAVs: First return on experience*. s.l., IEEE.
- Gobel, J. & Krzesinski, A. E., 2008. *A Model of Autonomous Motion in Ad Hoc Networks to Maximise Area Coverage*. Adelaide, Australia, IEEE.
- Howard, A., Mataric, M. J. & Sukhatme, G. S., 2002. *Mobile Sensor Network Deployment using Potential Fields: A Distributed, Scalable Solution to the Area Coverage Problem*. Fukuoka, Japan, Springer.
- Jaimes, A., Kota, S. & Gomez, J., 2008. *An approach to surveillance an area using swarm of fixed wing and quad-rotor unmanned aerial vehicles UAV(s)*. s.l., IEEE.
- Jin, J., Adrian, G. & Gans, N., 2014. *A Stable Switched-System Approach to Obstacle Avoidance for Mobile Robots in SE(2)*. Chicago, IL, USA, IEEE, pp. 1533-1539.
- Khatib, O., 1986. Real-Time Obstacle Avoidance for Manipulators and Mobile Robots. *The International Journal of Robotics*, 03 01, 5(1), pp. 90-98.
- Riley, G. F. & Henderson, T. R., 2010. The ns-3 Network Simulator. Dans: K. Wehrle, M. Güneş & J. Gross, eds. *Modeling and Tools for Network Simulation*. s.l.:Springer Berlin Heidelberg, pp. 15-34.
- To, L., Bati, A. & Hillard, D., 2009. *Radar Cross Section measurements of small Unmanned Air Vehicle Systems in non-cooperative field environments*. s.l., IEEE, pp. 3637-3641.
- Varga, A., 2001. *The OMNeT++ discrete event simulation system*. Prague, Czech Republic, s.n., pp. 319-324.